Spatial and temporal variability of nitrogen load from catchment and retention along a river network: a case study in the upper Xin'anjiang catchment of China

Ai Wang, Lihua Tang and Dawen Yang

ABSTRACT

Understanding the spatial and temporal variability of nitrogen load and characteristics of retention along a river network is important for land management and water resources protection. This study employs a geomorphology-based non-point source pollution model (GBNP) to simulate the hillslope hydrological processes and transport of sediment and pollutants in the upper Xin'anjiang (XAJ) catchment. Based on the simulation, the spatial and temporal distribution of total nitrogen (TN) load from hillslopes and retention characteristics along the river network are analyzed. The results indicate that annual TN load ranges from 0.54 ton/km^2 to 1.88 ton/km^2 and is relatively higher during spring and summer. Average TN load positively correlates with irrigated cropland area ($r = 0.820$) and negatively correlates with forest ($r = -0.43$). Seasonal TN retention ratios in the river network range from 0% to 81%, and streams of order 1 in the Horton–Strahler system have the highest retention ratio and are followed by orders 2, 3, and 4, which are mainly determined by the river hydraulic properties. Results of scenarios analysis demonstrate that TN retention ratios in the river network increase with TN load from hillslopes, but reach a maximum value rapidly, which indicates the limitation of the self-purification capacity of rivers.

Key words | geomorphology based non-point source pollution model, non-point load from catchment, total nitrogen retention along river network, Xin'anjiang catchment

Ai Wang
Lihua Tang (corresponding author)
Dawen Yang
State Key Laboratory of Hydroscience and Engineering,
Department of Hydraulic Engineering,
Tsinghua University,
Beijing,
100084,
China
E-mail: *tanglh@tsinghua.edu.cn*

INTRODUCTION

Non-point source (NPS) pollution is the major source causing river and lake eutrophication and has become the largest threat to water quality in recent years. It has been estimated that 30–50% of surface water bodies in the world have been affected by NPS pollutants (Pimentel 1993) and NPS has been a major cause of water quality problems (Ongley *et al.* 2010; Collick *et al.* 2015). In China, the NPS contribution to water pollution has ranged up to 81% from nitrogen (N) and 93% from phosphorus (P) (Ongley *et al.* 2010). Compared with point source pollution, NPS pollutants have higher variabilities in space and time, and are relatively easy to deposit and degrade along a river network. Understanding the characteristics of nutrient load over a catchment and retention in river networks is important for land management and water quality protection.

Nutrient pathway in a catchment can be classified into two distinctly different but interactional components, i.e., terrestrial landscape and river network. Both components involve the interactions of hydrological processes with biogeochemical and ecological processes on land and in the river network (Ye *et al.* 2012). It is practically difficult to observe NPS total nitrogen (TN) load from hillslopes and retention along a river network at catchment scale. Alternatively, researchers have attempted to develop appropriate models to simulate such processes in a catchment. There are several distributed models of NPS pollution, such as

doi: 10.2166/nh.2015.055

Downloaded from https://iwaponline.com/hr/article-pdf/47/4/869/368357/nh0470869.pdf
by guest
on 14 August 2018

hydrological simulation program-Fortran (HSPF) (Bicknell *et al.* 1997), agricultural non-point source (AGNPS) (Young *et al.* 1989), and soil and water assessment tool (SWAT) (Borah & Bera 2004). However, the discretization of the watershed (e.g., hydrologic research units (HRUs) used in a SWAT model) and the equations used for description of all these processes (e.g., soil conservation service (SCS) curve method used in SWAT and the universal soil loss equation (USLE) used in AGNPS model) are different, which may cause different application effects in different basins. The geomorphology-based non-point source pollution model (GBNP) (Tang *et al.* 2011) discretizes a watershed into 'hillslope–river network' and describes the dynamics of pollutant transport and relevant hydrology and hydraulics. It has been successfully applied to the Chaobai River basin in North China to simulate the effect of land use change on streamflow, sediment, and nutrient losses (Tang *et al.* 2011).

Previous studies have paid more attention to the factors that may influence NPS pollution load from different catchments. Researchers have proved that factors such as soil characteristics (Ouyang *et al.* 2009; Shen *et al.* 2013), rainfall intensity (Shen *et al.* 2012, 2014; Wu *et al.* 2012), vegetation (Ouyang *et al.* 2009), land use and land cover (Wu *et al.* 2012) affect water quantity and quality in rivers. Several studies focused on NPS loads from particular land use types, especially from agricultural land use-dominated catchments (Esen & Uslu 2008; Somura *et al.* 2012) or from forest-dominated catchments (McBroom *et al.* 2008).

The level of N and P coming from a catchment to a river outlet can be decreased through riverine retention processes (Chen *et al.* 2010), and this is the result of sediment sorption, plant and microbial uptake, and denitrification (Saunders & Kalff 2001; Alexander *et al.* 2007; Ye *et al.* 2012). However, N and P retention by adsorption and degradation may vary along a river network and from one catchment to another (Svendsen & Kronvang 1993; Kronvang *et al.* 1999; Chen *et al.* 2010). Different factors may affect nutrient retention: (1) river channel characteristics, e.g., channel length, grade, and size (Peterson *et al.* 2001; Alexander *et al.* 2007; Mulholland *et al.* 2008; Covino *et al.* 2010a, 2010b; McNamara 2010); (2) flow condition, e.g., discharge, flow velocity, and water depth (Spieles & Mitsch 1999; Seitzinger *et al.* 2002; Grizzetti *et al.* 2003; Rankinen *et al.* 2014); and (3) some other factors that influence vegetation condition, such as dissolved oxygen, temperature, and sunshine hours (Chen *et al.* 2010, 2013). Although many studies focused on either nutrient load from the terrestrial landscape or transport and degradation in a river network, not much work has been done to analyze the two processes together at catchment scale. There is still a knowledge gap in understanding the relationship between NPS nutrient load from landscape and its fate during the transport process along the river network.

Xin'anjiang (XAJ) catchment is the major source of drinking water for Hangzhou city (Figure 1) of Zhejiang Province. Protection of headwaters is a key issue for Hangzhou city. However, the headwaters are located in Anhui Province. In order to solve the conflict between economic development and environmental protection, the Ministry of Environmental Protection of China has selected the upper XAJ catchment as the first 'Ecological Compensation Pilot Catchment' since 2010. To carry out the ecological compensation in this catchment, it is important to know the temporal and spatial variability in both runoff (the major water resource) and the pollutants load over the catchment and along the river network.

This study adopts the GBNP model to simulate TN transport processes in the XAJ catchment during the recent 10 years from 2001 to 2010. The main objectives include: (1) to estimate the spatio-temporal variation of TN load from the landscape and to analyze the controlling factors; (2) to understand the seasonal variations of TN retention in streams along the river network from upstream to downstream and the effects of hydro-morphological properties on TN retention ratios; and (3) to explore the relationships between NPS TN load and river retention.

STUDY AREA AND DATA

Study area

The XAJ catchment is situated in southeast China with an area of approximately 11,700 km^2 across both Anhui and Zhejiang Provinces. In this study the headwater region located in Anhui Province is selected as the study area, which has an area of 5,899 km^2, covering about 54% of the XAJ catchment (see Figure 1). The study catchment is located in the subtropical, humid monsoon climate zone with a mean annual

Downloaded from https://iwaponline.com/hr/article-pdf/47/4/869/368357/nh0470869.pdf
by guest
on 14 August 2018

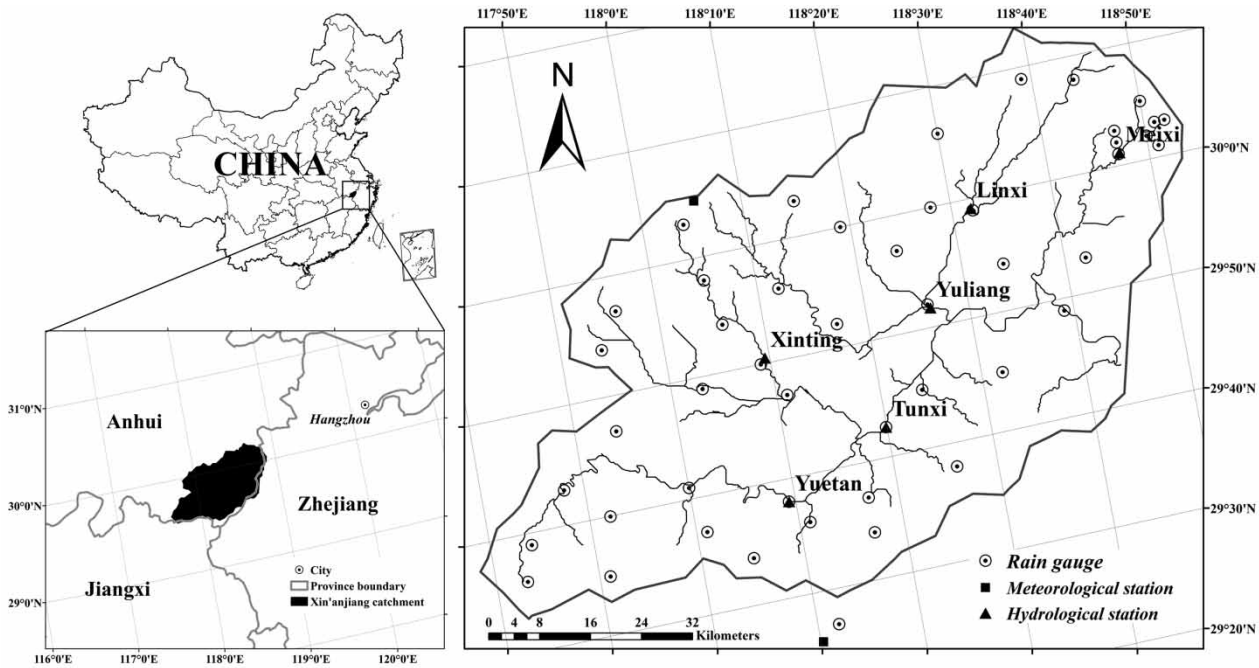

Figure 1 | Location of study catchment and locations of rain gauges, meteorological station, and hydrological station.

temperature of 15.5 °C and a mean annual precipitation of 1,752 mm (Zhai *et al.* 2014). Precipitation varies spatially and temporally, and falls predominantly between April and July. Elevation in this catchment ranges from approximately 130 to 1,600 m. About 68% of the catchment area is covered by forest, the dominant types being evergreen broad-leaf forest and deciduous and evergreen broadleaved forest. Agricultural farmlands take up about 19% of the catchment area and the major crops are rice and winter wheat. The remaining land use types include mainly wetland, grassland, and urban areas (see Figure 2). The major soil types in this catchment are ferralsol, paddy soil and purple soil, 62.4%, 14.6%, and 9.8%, respectively (Li *et al.* 2015). Ferralsol is easily eroded and has low storage and water supply capacity (Zhai *et al.* 2014).

The study area is located in the uncovered bedrocks area. The landform undulates greatly and hydrogeological condition is simple. Precipitation is the main source of groundwater and the depth of groundwater ranges from 5 m to 10 m. Most of the groundwater quality is good (Liu 2009). Owing to agricultural activities, the quality of the surface water environment has deteriorated in recent years (Ye & Wu 2005). The NPS pollutants load increased from 2001 to 2010 (Zhai *et al.* 2014). In 2010, the total amount of TN, total phosphorus (TP), and chemical oxygen demand (COD_{cr}) was reported to be 13,400 ton, of which TN and TP accounted for about 59% and 6%, respectively (Wang *et al.* 2012). TN load from hillslope is mainly affected by land use types (Wang *et al.* 2014). Rice planting yielded the most pollutants (TN and TP), followed by tea gardens and winter wheat (Zhai *et al.* 2014).

Data used

Topography, land use, soil type, and vegetation are the basic geographical information that is used to build the GBNP model. Digital elevation data were obtained from the US Geological Survey (http://hydrosheds.cr.usgs.gov/datasource.php) with a 30 m spatial resolution. Land use data were obtained from the Environmental and Ecological Science Data Center for West China (EESD) (http://westdc.westgis.ac.cn/), and were re-grouped into the following eight categories: water bodies, urban area, forest, irrigated cropland, upland, grassland, shrub, and wetland (Figure 2), with a 100 m spatial resolution. The distributed soil hydraulic parameters of the van Genuchten equation were obtained from the Land–Atmosphere Interaction Research Group at Beijing Normal

Downloaded from https://iwaponline.com/hr/article-pdf/47/4/869/368357/nh0470869.pdf
by guest
on 14 August 2018

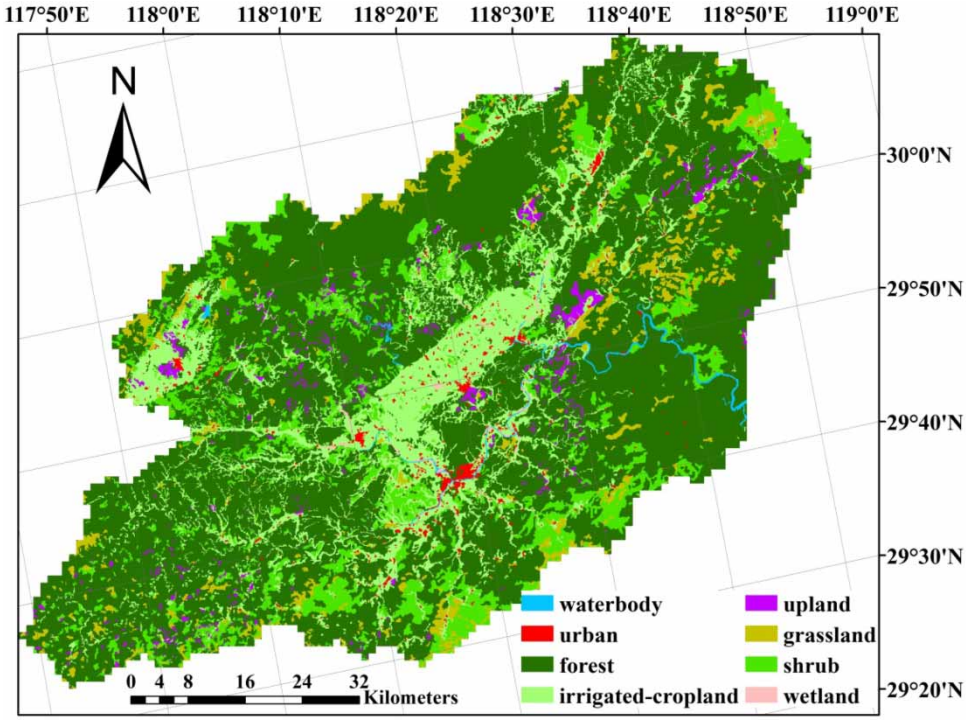

Figure 2 | Land use of the study catchment.

University (http://globalchange.bnu.edu.cn/research/soil3) (Dai *et al.* 2013), and comprise saturated water content (θ_s), residual moisture content (θ_r), inverse of the air-entry pressure (α), shape parameter (n), the saturated hydraulic conductivity (K_s), with a 0.00833° (about 900 m) spatial resolution. Soil chemical properties were obtained from the Institute of Soil Science, Chinese Academy of Sciences (http://www.soil.csdb.cn/). Monthly NDVI (Normal Differential Vegetation Index) data were obtained from SPOT (Système Probatoire d'Observation de la Terre) and were observed three times a month.

Daily precipitation data at 48 rain gauges were collected from the Huangshan Hydrographic Bureau. Daily meteorological data, including precipitation, wind speed, relative humidity, hours of sunshine, as well as maximum, minimum, and mean air temperatures at two stations (Tunxi and Huangshan) were obtained from China Meteorological Administration. The data set span was over the period from 2001 to 2010. Monthly discharge data at six hydrological stations (Tunxi, Yuliang, Meixi, Linxi, Yuetan, Xinting) were obtained from the *Hydrological Year Book* published by the Hydrological Bureau of the Ministry of Water Resources. Monthly water quality data, including sediment yield and TN concentration at Tunxi and Yuliang stations, were obtained from the Huangshan Hydrographic Bureau. Monthly discharge data covered the time period from 2001 to 2010, and monthly water quality data covered the period from 2003 to 2010. The locations of rain gauges, meteorological stations, and hydrological stations are shown in Figure 1.

Non-point pollutant sources considered in this study include fertilization, rural domestic water and effluents from livestock and poultry. The related social economic data were obtained from the Statistics Office of Huangshan (2011). Point pollutant sources, including waste water discharges from industries and sewage treatment plants were obtained from the Huangshan Hydrographic Bureau.

METHODOLOGY

Brief introduction of GBNP model

The GBNP model was developed on the basis of the geomorphology-based hydrological model (GBHM)

Downloaded from https://iwaponline.com/hr/article-pdf/47/4/869/368357/nh0470869.pdf
by guest
on 14 August 2018

(Yang *et al.* 1998, 2002), which has been successfully applied to the Yellow River basin and Yangtze River Basin of China (Xu *et al.* 2008; Cong *et al.* 2009) to simulate the hillslope hydrological processes and flow routing in river networks. In order to represent topographical and landscape characteristics effectively, the GBNP used the same discretization method and sub-grid parameterization scheme as in the GBHM. First, the catchment boundary is extracted from the digital elevation model (DEM) of 30 m × 30 m resolution, and then the catchment is divided into several sub-catchments (in this study, the XAJ catchment is divided into 77 sub-catchments) and the steam network is generated and ranked by the Horton–Strahler classification system (in this study the steam network has four orders; see Figure 3). In each sub-catchment the stream pathway is simplified by using a single main channel that has the maximum flow length of this sub-catchment. The runoff generated from each grid over the sub-catchment is assumed to be the lateral inflow of the main channel (Yang *et al.* 2015). According to the data resolution and computation efficiency, 1-km × 1-km grid system is resampled from the original DEM, land use, and soil maps. Each 1-km × 1-km grid is represented by a number of topographically similar 'hillslope–valley' systems, and is the basic unit of the hydrological simulation.

In the GBHM, hillslope hydrological processes include snowmelt, canopy interception, evapotranspiration, infiltration, surface flow, subsurface flow and exchange between groundwater and river. Snowmelt is calculated using the temperature-index approach. The actual evapotranspiration is calculated from the potential evaporation by considering seasonal variation of LAI, root distribution, and soil moisture availability. Infiltration and soil water flow in the vertical direction of the hillslope is simulated using the Richards' equation. The surface runoff is from the infiltration excess or saturation excess and flows through the hillslope into the stream. The groundwater aquifer is treated as an individual storage corresponding to each grid. Exchange between the groundwater flow and river water is calculated by Darcy's law, and this is especially important in mountain hydrology. Flow routing in the river network is solved using kinematic wave approach. More details about these processes can be referred to in Yang *et al.* (2002).

The GBNP model couples soil erosion and nutrient transportation into GBHM to simulate the NPS pollution processes

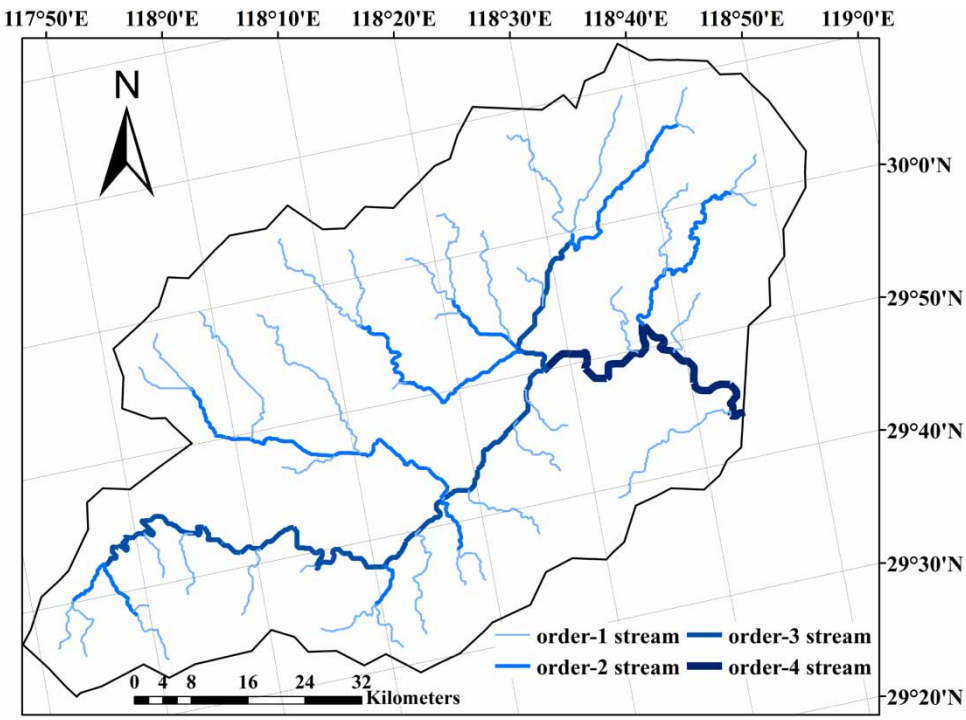

Figure 3 | River networks of the study catchment ordered by the Horton–Strahler system.

Downloaded from https://iwaponline.com/hr/article-pdf/47/4/869/368357/nh0470869.pdf
by guest
on 14 August 2018

in a catchment. On a hillslope, soil erosion and nutrient (i.e., nitrate, ammonia, and organic nitrogen in this study) dynamics are incorporated with the rainfall–runoff processes. In the river network, sediment transport, dissolved (nitrate) and absorbed (ammonia and organic N) N are simulated together with flow routing. The main processes are shown in Figure 4.

Pollutants' transport on hillslope

Sediment eroded from hillslope can be flushed into the river by surface flow. Soil erosion on a hillslope is estimated using the mass conservation equation considering both rill and inter-rill erosions (Bennett 1974). The pollutants can be transported into the river by water flow and sediment movement. In a hillslope grid, pollutants' transportation during the rainfall process is simulated in three layers: moving with runoff or sediment along the hillslope, exchange between runoff and soil in a mixed layer, and vertical leaching in lower soil profile (Gao *et al.* 2004). All these transportation processes are calculated by mass conservation equations. More details can be referred to in Tang *et al.* (2011). The depth of mixed layer is decided by rainfall intensity, soil properties, and agrotechnical actions.

Nitrate leaching is reported to be one of the most important factors causing groundwater pollution (Libra & Hallberg 1998; Aravena *et al.* 1999) because of the contrary electrode with soil particle. The vertical movement of pollutant in the unsaturated soil profile is represented by the convection–dispersion equation (CDE) (Biggar & Neilsen 1962, 1963; Neilsen & Biggar 1961, 1962):

$$\frac{\partial(C_L+\rho C_s)}{\partial t}+\frac{\partial(vC_L)}{\partial z}=\frac{\partial}{\partial z}(\theta\cdot D\cdot\frac{\partial C_L}{\partial z}+\Phi) \quad (1)$$

where C_L is the liquid pollutant concentration, kg m^{-3}; C_s is the solid absorption concentration, kg kg^{-1}, and $C_s = K_d \cdot C_L$, where K_d is the solid liquid distribution coefficient, m^3 kg^{-1}; v is the discharge velocity, m s^{-1}; D is hydrodynamic dispersion coefficient, m^2 s^{-1}; ρ is soil bulk density, kg m^{-3}; Φ is the term for the source or sink in soil profile, kg m^{-3} s^{-1}; z is the depth of soil profile, m; θ is soil volumetric moisture content at the moment t of the depth z.

The source or sink during the time of dt can be calculated as follows:

$$\Phi\cdot V\cdot dt = M_{\text{fer}}+M_{\text{min}}-M_{\text{tran}}-M_{\text{uptake}}-M_{\text{runoff}}+M_i \quad (2)$$

where V is the soil volume, m^3; M_{fer} is surface soil pollutant amount coming from fertilization, kg; M_{min} is mineralization amount coming from soil humus or plant residues, kg; M_{tran} is the transfer quantity between different forms of N, kg, which contains mineralization (from organic nitrogen to ammonia), nitrification (from ammonia to nitrate nitrogen),

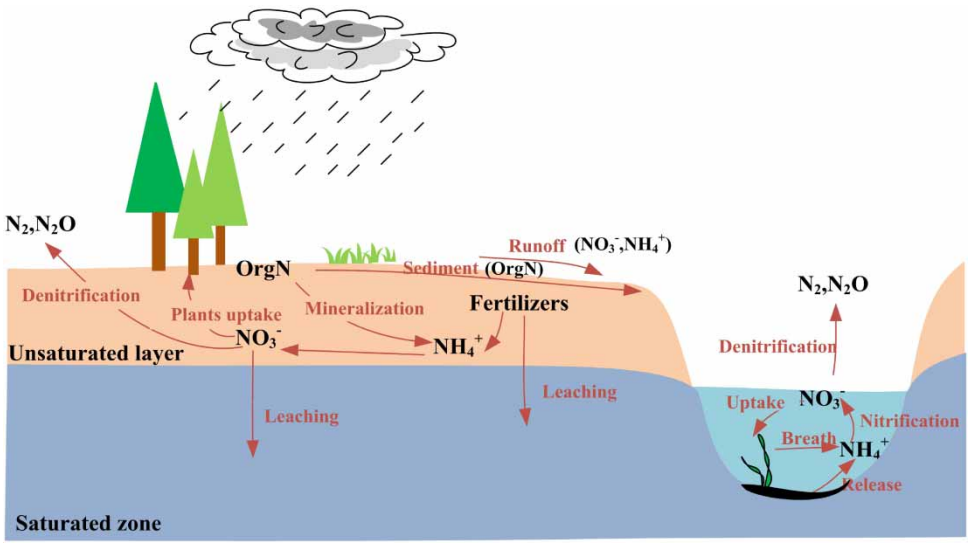

Figure 4 | Transformations between different forms of nitrogen in the soil profile and river segment described in the GBNP model.

Downloaded from https://iwaponline.com/hr/article-pdf/47/4/869/368357/nh0470869.pdf
by guest
on 14 August 2018

and denitrification (from nitrate to nitrogen oxides or gas) and can be calculated by the first-order kinetics equation $\varphi_i = -\mu_i C_i$, where φ_i is the transfer amount of form i, C_i is the amount of form i, μ_i is the reaction coefficient, which is affected by soil temperature, water content, and oxygen concentration; M_{uptake} is the amount of crop root uptake which is calculated by Watts and Hanks's function (Watts & Hanks 1978), kg; M_{runoff} is the losses during runoff or subsurface flow, kg; M_i is atmospheric wet deposition of N (nitrate and ammonia N), kg; and $M_i = r \cdot P \cdot A$, where r is the content of pollutant in the rain, mg L^{-1}, P is daily precipitation, mm, A is surface area of hillslope, m^2. However, r is a varied value in different seasons, and connected with precipitation, wind direction, location, etc. (Zhang *et al.* 2003). Owing to lack of observation, in this paper a single value of r was used for the whole catchment in the whole period, which was taken from Environmental Monitor Station of Huangshan (2011).

Some nitrate may leach from soil into the groundwater. Pollutants' transport in the groundwater is a long-term process. A simplified lumped groundwater quality model is adopted to descript this process as follows:

$$ph\frac{dC}{dt} + (q_r + aph)C = q_r C_r \tag{3}$$

where C is pollutant concentration in groundwater, kg m^{-3}; C_r is the pollutant concentration of unsaturated seepage, kg m^{-3}; h is the average depth of saturated zone, m; p is the average effective porosity; q_r is the natural leak rate, m s^{-1}; a is the first order reaction constant of pollutants' attenuation.

Pollutants' transport in river network

Sediment transport in a river segment is calculated using a one-dimensional equation (Wang & Hu 2006). It considers both sediment settling and bank erosion but ignores sediment diffusion. The absorbed nutrients (organic nitrogen) movement process can be calculated as follows (Yu *et al.* 2006):

$$C_{\text{sed}}\frac{\partial(AC_{\text{sorb}})}{\partial t} + C_{\text{sed}}\frac{\partial(QC_{\text{sorb}})}{\partial x} - \frac{\partial}{\partial x}\left(AE_x\frac{\partial(C_{\text{sed}}C_{\text{sorb}})}{\partial x}\right) = q_l C_{\text{sorbl}} C_{\text{sedl}} + \alpha\omega B(C_{\text{sed}}* - C_{\text{sed}})(C_k - C_{\text{sorb}}) \tag{4}$$

where C_{sed} is sediment concentration, kg m^{-3}; C_{sorb} is the absorbed pollutants' concentration, kg m^{-3}; x denotes length along water flow direction, m; Q is the river discharge, $m^3\ s^{-1}$; E_x is the longitudinal dispersion coefficient, $m^2\ s^{-1}$; C_{sorbl} is the absorbed nutrient concentration in lateral runoff, kg kg^{-1}; C_{sedl} is the sediment concentration in lateral runoff, kg m^{-3}; C_k is the nutrient concentration of the sediment on riverbed, kg m^{-3}; $C_{\text{sed}}*$ is the sediment carrying capacity, kg m^{-3}; α is the recovery saturation coefficient; ω is the settling velocity of sediment, m s^{-1}; B is the river width, m; A is the wet section area, m^2; q_l is the lateral inflow from the hillslope per unit width, $m^2\ s^{-1}$.

The movement of dissolved pollutants (nitrate and ammonia nitrogen) in a river segment is represented by the longitudinal dispersion equation (Chu 1994; Yu *et al.* 2006):

$$\frac{\partial(AC_{\text{dis}})}{\partial t} + \frac{\partial(QC_{\text{dis}})}{\partial x} = \frac{\partial}{\partial x}\left(AE_x\frac{\partial C_{\text{dis}}}{\partial x}\right) + S \tag{5}$$

where C_{dis} is the dissolved pollutant concentration in the river, kg m^{-3}; S is the term for the source or sink in the river, including pollutants flowing in from the lateral hillslopes, and released from the bottom mud or transformed by bio-chemical interaction (nitrification, denitrification), kg $m^{-1}s^{-1}$; A is wetted area, m^2.

The nitrate source or sink S_{NO_3} is calculated as (Brown & Barnwell 1987):

$$S_{NO_3} = \frac{M_{NO_3}}{dx} + K_{n,1}\cdot C_{NH_3}\cdot A - K_{n,2}\cdot C_{NO_3}\cdot A - \alpha_1\cdot C_{NO_3}\cdot A \tag{6}$$

where M_{NO_3} is the nitrate amount coming from lateral flow, including surface flow, subsurface flow, and groundwater, kg; C_{NO_3} is nitrate concentration in the river, kg m^{-3}; C_{NH_3} is the ammonia concentration in the river, kg m^{-3}; $K_{n,1}$ is nitrification coefficient, day^{-1}; $K_{n,2}$ is denitrification coefficient, day^{-1}; α_1 is attenuation coefficient for the uptake by water-weed, day^{-1}; A is the wet section area, m^2.

The ammonia source or sink S_{NH_3} is calculated as (Brown & Barnwell 1987):

$$S_{NH_3} = \frac{M_{NH_3}}{dx} + K_{n,3}\cdot C_{orgN}\cdot A + S_r\frac{A}{h} - K_{n,1}\cdot C_{NH_3}\cdot A \tag{7}$$

Downloaded from https://iwaponline.com/hr/article-pdf/47/4/869/368357/nh0470869.pdf
by guest
on 14 August 2018

where M_{NH_3} is the nitrate amount coming from lateral flow, including surface flow, subsurface flow, and groundwater, kg; C_{orgN} is the organic TN concentration, kg m^{-3}; $K_{n,3}$ is the mineralization coefficient, day^{-1}; S_r is ammonia release rate from sediment, kg $m^{-2}day^{-1}$; h is water depth, m.

Through the previous processes, the nitrogen loads (including nitrate, ammonia, and organic nitrogen) from the hillslope of each grid and the concentrations of nitrate, ammonia, and organic nitrogen in the river network can be calculated.

Model calibration and validation

The main parameters of the GBNP model are listed in Table 1. Based on the available data, the monthly discharges of 2001–2003 at six hydrological stations, namely, Tunxi, Yuliang, Meixi, Linxi, Yuetan, and Xinting are used for calibrating the hydrological module, and the monthly discharges of 2004–2010 were used for validation. The monthly sediment and TN concentrations at Tunxi and Yuliang stations in the period 2003–2005 are used for calibration of sediment and TN module while the monthly data of 2006–2010 are used for validation. All those parameters are calibrated through trial and error.

The Nash–Sutcliffe coefficient of efficiency (E_{ns}) and coefficient of determination (R^2) are used to evaluate the model performance:

$$E_{ns} = 1.0 - \frac{\sum_{i=1}^{n} (Q_{si} - Q_{oi})^2}{\sum_{i=1}^{n} (Q_{oi} - \overline{Q_o})^2} \tag{8}$$

$$R^2 = \frac{\sum_{i=1}^{n} (Q_{si} - \overline{Q_s})(Q_{oi} - \overline{Q_o})}{\sqrt{\sum_{i=1}^{n} (Q_{oi} - \overline{Q_o})^2} \sqrt{\sum_{i=1}^{n} (Q_{si} - \overline{Q_s})^2}} \tag{9}$$

where Q_{si} is simulation value, $\bar{Q}_s$ is average value of simulation, Q_{oi} is observation value, $\bar{Q}_o$ is average value of observation.

Table 1 | Main parameters used in the GBNP

Parameter	Method of estimation	Value range
Hydrological parameters	Refer to Ma *et al.* (2010)	
Erosion and sediment routing parameters		
Inter-rill and rill erosion capability	Estimated according to soil type and land use using an empirical function of rain intensity, slope, soil erodibility and factor of agricultural management	Inter-rill erosion capability [0,0.0001] $kg/m^2/s$. Rill erosion capability [0,150] $kg/m^2/s$
Soil erodibility	Estimated for each soil type according to the soil database of China	[0.09,0.50]
Parameters in the calculation of sediment-carrying capacity, K and m	Estimated by a function of flow velocity, hydraulic radius, and settling velocity of sediment	K = [0.025,0.20]. M = [0.92,1.20]
Sediment settling velocity	Estimated by particle diameter of suspended sediment and flow velocity	[0.01,0.08] m/s
Coefficient of saturation recovery	Calibration for each river segment	[0.25,1.00]
Pollutant parameters		
Longitudinal dispersive coefficient in river	Calibration for each river segment	[50,500] m^2/s
Residue decomposition coefficient	Estimated according to land use type	[0.00018,0.0036] kg N/ha
Release rate of bottom mud and bio-chemical interaction	Calibration for each river segment	[0.0005,0.001] 1/h
Other parameters		
Exchange layer depth	Calibration for each subbasin	[0.1,0.2] m
Water release rate from soil to runoff	Estimated by a function of soil erodibility, rain intensity	[0.00001,0.016] m/h

Downloaded from https://iwaponline.com/hr/article-pdf/47/4/869/368357/nh0470869.pdf
by guest
on 14 August 2018

As shown in Table 2, it can be seen that the values of R^2 are greater than 0.9 for monthly discharge and sediment load, and are greater than 0.8 for monthly TN load. The values of E_{ns} for monthly discharge are greater than 0.8 except for the validation period at the Linxi and Yuliang stations. The values of E_{ns} for monthly sediment and TN are relatively lower (the smallest value is 0.58), which may be caused by the error accumulation and observation frequency. In addition, as mentioned before, the source of pollutants may come from statistical data, thus the uncertainty of inputs leads to the uncertainty of results.

Stream TN retention analysis

In this research, TN retention in a stream segment is defined as the TN reduction mainly including intake by biomass (i.e., uptake) and removal by microorganisms (i.e., denitrification), which can be estimated by the difference between the input and output of TN. The TN inputs may come from the upstream, the hillslopes along the stream and waste water as point sources discharged into the stream and can be expressed as:

$$R_i = M_{\text{in},i} + M_{\text{hill},i} + M_{\text{point},i} - M_{\text{out},i} \tag{10}$$

where R_i is TN retention of river segment i, when $R_i > 0$, this segment is a sink of TN, otherwise it is a source; $M_{\text{in},i}$ is TN input from river segment *i-1*; $M_{\text{hill},i}$ is TN input from hillslope of this segment; $M_{\text{point},i}$ is point source pollution in this segment; $M_{\text{out},i}$ is TN output of segment *i*. All quantities can be expressed as a weight (e.g., kg), and all of them are monthly data.

The retention ratio η is defined as:

$$\eta = 1 - \frac{M_{\text{out},i}}{M_{\text{in},i} + M_{\text{hill},i} + M_{\text{point},i}} \tag{11}$$

RESULTS

Spatio-temporal variation of TN load from hillslope

The annual TN load from the hillslopes during 2001–2010 are illustrated in Figure 5, which ranges from 3,156 ton (0.54 ton/km^2) to 11,079 ton (1.88 ton/km^2) with a significant increasing trend. However, meanwhile, the annual precipitation has no obvious trend in this period. The correlation between simulated TN load with monthly discharge and sediment load from 2001 to 2010 is shown in Figure 6. It demonstrates that TN load has a significant positive correlation with both discharge and sediment. The correlation coefficient between annual TN load and annual mean discharge and between annual TN load and annual sediment load are 0.91 and 0.85, respectively.

Comparing the mean monthly TN load with the monthly discharge and sediment load in these 10 years (Figure 7), the monthly TN load and sediment load changes together with the river discharge. It is obvious that TN load

Table 2 | Model calibration and validation based on the monthly simulations

		R^2		E_{ns}	
Name of the hydrological gauge	**Item**	**Calibration period**	**Validation period**	**Calibration period**	**Validation period**
Yuetan	Discharge	0.97	0.97	0.95	0.95
Xinting	Discharge	0.94	0.96	0.88	0.86
Tunxi	Discharge	0.97	0.98	0.92	0.95
	Sediment	0.97	0.93	0.91	0.85
	TN	0.82	0.81	0.65	0.58
Linxi	Discharge	0.95	0.93	0.89	0.73
Meixi	Discharge	0.97	0.97	0.95	0.94
Yuliang	Discharge	0.95	0.94	0.83	0.65
	Sediment	0.92	0.93	0.71	0.68
	TN	0.88	0.88	0.72	0.59

Downloaded from https://iwaponline.com/hr/article-pdf/47/4/869/368357/nh0470869.pdf
by guest
on 14 August 2018

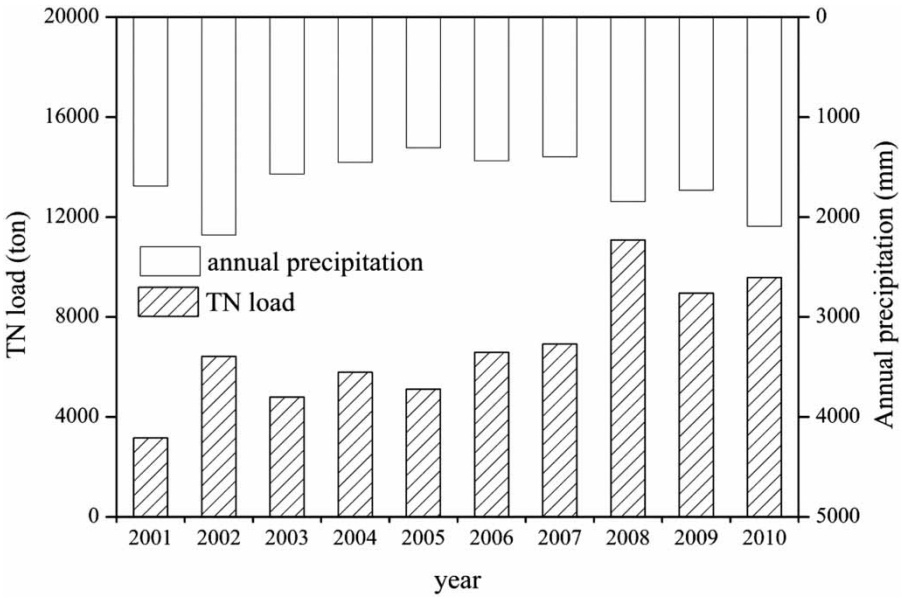

Figure 5 | Change of the annual TN load from 2001 to 2010 in the study catchment.

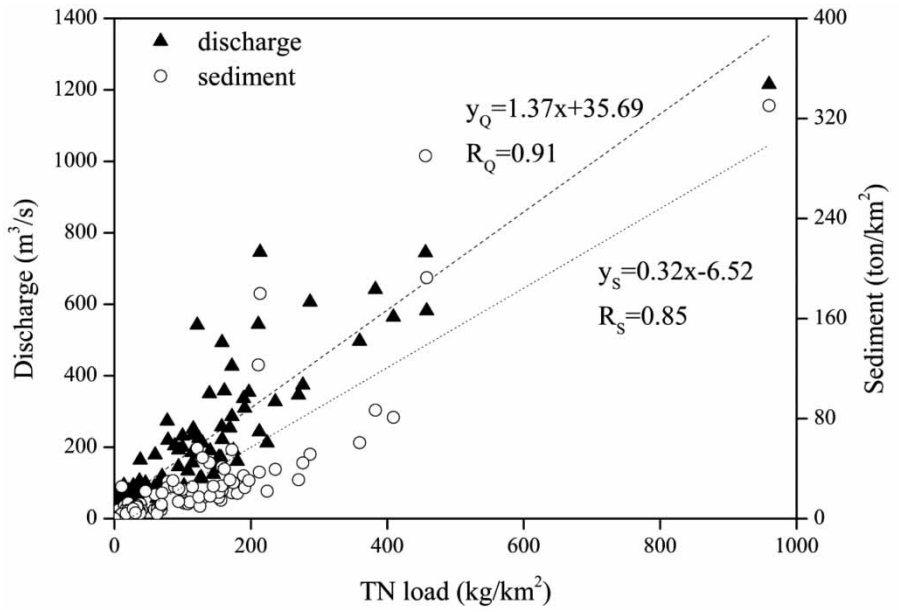

Figure 6 | Correlation between TN load and discharge and sediment.

is relatively higher in spring (435.30 kg/km^2) and summer (487.84 kg/km^2), while it is lower in autumn (97.72 kg/km^2) and winter (138.34 kg/km^2) (spring: from March to May; summer: from June to August; autumn: from September to November; winter: from December to February). In addition, the TN load is higher in winter compared with the TN load in autumn.

The spatial distribution of the seasonal TN load is illustrated in Figure 8; it is also demonstrated that spring and summer are the major seasons for TN

Downloaded from https://iwaponline.com/hr/article-pdf/47/4/869/368357/nh0470869.pdf
by guest
on 14 August 2018

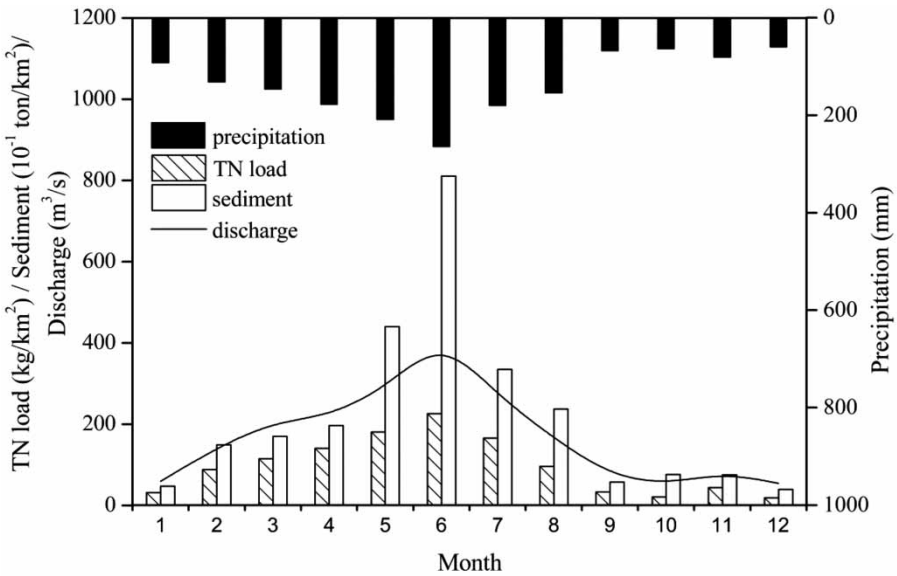

Figure 7 | Comparison of the monthly TN load with the monthly discharge and sediment from 2001 to 2010 in the study catchment.

load. The highest TN load occurs in the central region of the study catchment, where the major land use type is irrigated cropland. This implies that the irrigated cropland is the major source of TN load in this catchment.

TN retention along the river network

Besides biological factors, nutrient retention is mainly influenced by the river discharge, flow velocity, air temperature, nutrient inputs, and so on (Behrendt & Opitz 2000; Grizzetti *et al.* 2003; Mao *et al.* 2006). Rivers with the same stream order usually have analogous hydraulic conditions (river discharge, flow velocity, bed slope, river length, etc.); the nutrient retention may also have analogous behavior (Seitzinger *et al.* 2002). Based on the GBNP simulation results, TN retention in the streams of different orders was analyzed. Figure 9 shows the average retention ratios of the streams of the four successive orders in four seasons. The retention ratios range from 0% to 81% in the streams of this catchment. The highest retention ratio is found in the stream of order 1, followed by orders 2, 3, and 4. For the streams of the four successive orders, the highest retention ratio appears in summer, which is consistent with the results reported by other researchers (Grizzetti *et al.* 2003; Chen *et al.* 2013).

DISCUSSION

Control factors of TN load from hillslope

Figure 5 indicates that the TN load is not significantly affected by the total amount of annual precipitation. Further analysis of the daily precipitation shows that the increase of TN loads is probably caused by the increase of rainfall intensity. For example, the annual precipitation in 2002 and 2010 were almost the same; however, TN load in 2002 was less than that in 2010 (Figure 5). According to the accumulative probability distribution of the daily precipitation in Figure 10, there was only 1% of rainfalls larger than 30 mm in 2002, and only one rainfall event was larger than 60 mm. Nevertheless, in 2010, nearly 5% of rainfalls were larger than 30 mm and four rainfall events were larger than 60 mm. This indicated that the daily rainfall intensity in 2010 was larger than that in 2002, which led to higher TN load in 2010. Similarly, comparing 2010 to 2008, although the precipitation was larger in 2010, the heavy rainfall events (larger than 60 mm) were less than those in 2008. It could provide a suitable explanation for the highest TN load in 2008. In 2005, the annual precipitation (see Figure 5) and the rainfall intensity (see Figure 10) were both smaller than those in the other three listed years, therefore the TN load was also the smallest.

Downloaded from https://iwaponline.com/hr/article-pdf/47/4/869/368357/nh0470869.pdf
by guest
on 14 August 2018

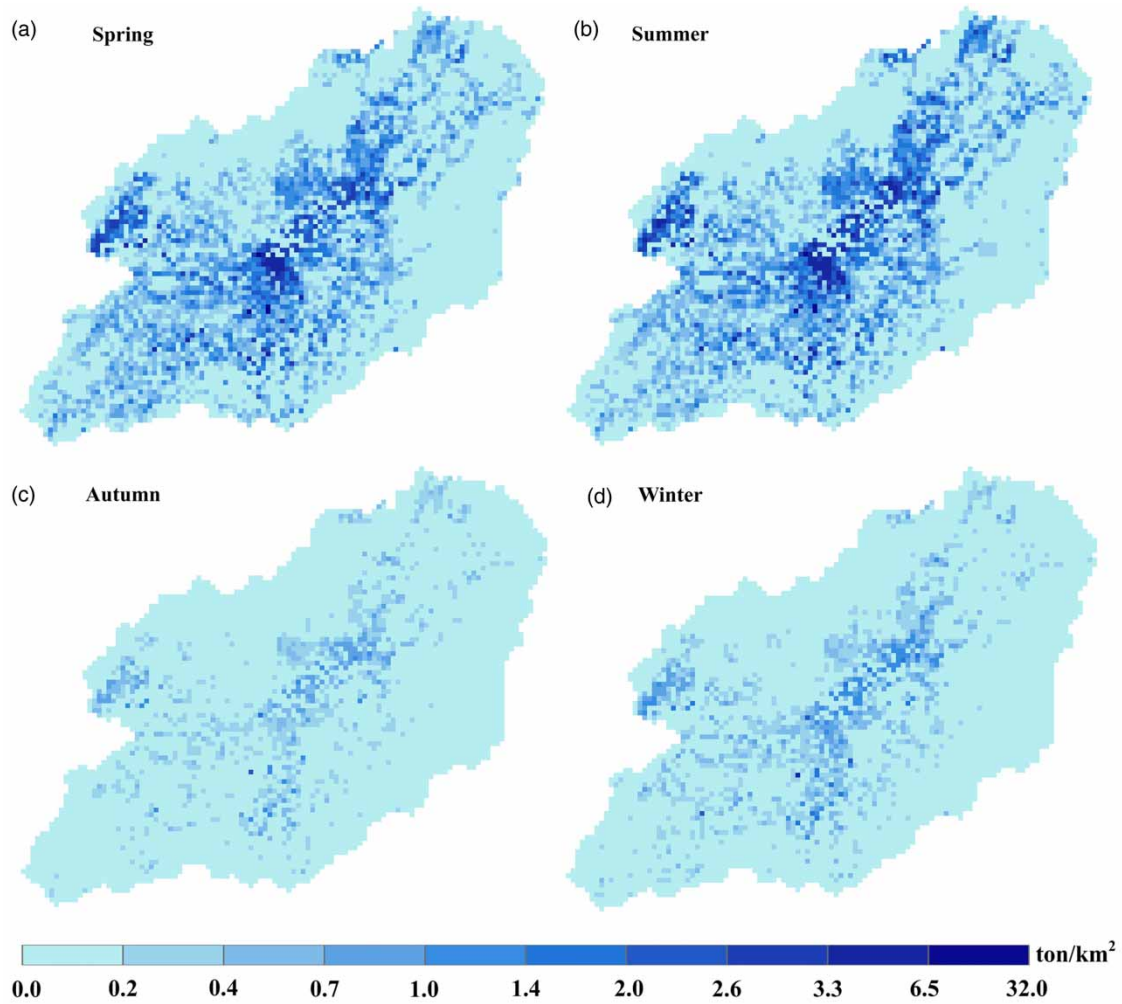

Figure 8 | Spatial and seasonal distributions of the 10-year mean TN load in the study catchment (seasonal average value in 10 years from 2001 to 2010).

For further proof, we selected two rainfall events in 2008 at Yuliang station, which have nearly the same total precipitation (117 mm from June 15th to June 20th, 124 mm from July 27th to August 3rd) but different rainfall intensity (Figure 11), and compared the daily TN load, sediment, and discharge. The results demonstrate that the first rainfall event produces more TN (156 ton) and sediment (518 10^2 ton) than the second one (TN: 80 ton, sediment: 201 10^2 ton) although the total precipitation is quite the opposite. According to the previous analysis, precipitation may affect TN load, but the critical factor is the rainfall intensity.

Table 3 gives the Pearson correlation between TN load and land use types. The average TN load has a significant positive correlation with the irrigated cropland area (Pearson correlation coefficient $r = 0.820$), and a significant negative correlation with the forest ($r = -0.43$) and grassland area ($r = -0.25$). This confirms that the major source of TN load in this catchment come from the irrigated cropland. This conclusion is also consistent with the result reported by Cao *et al.* (2013).

As well, agrotechnical actions are important for TN load from farmlands. We considered the influence of agrotechnical actions on TN load by: (1) introducing a farmland surface storage for calculation of surface flow; (2) a crop management factor for erosion estimation; (3) a depth of mixed layer for pollutants' transportation; and (4) fertilization time.

Downloaded from https://iwaponline.com/hr/article-pdf/47/4/869/368357/nh0470869.pdf
by guest
on 14 August 2018

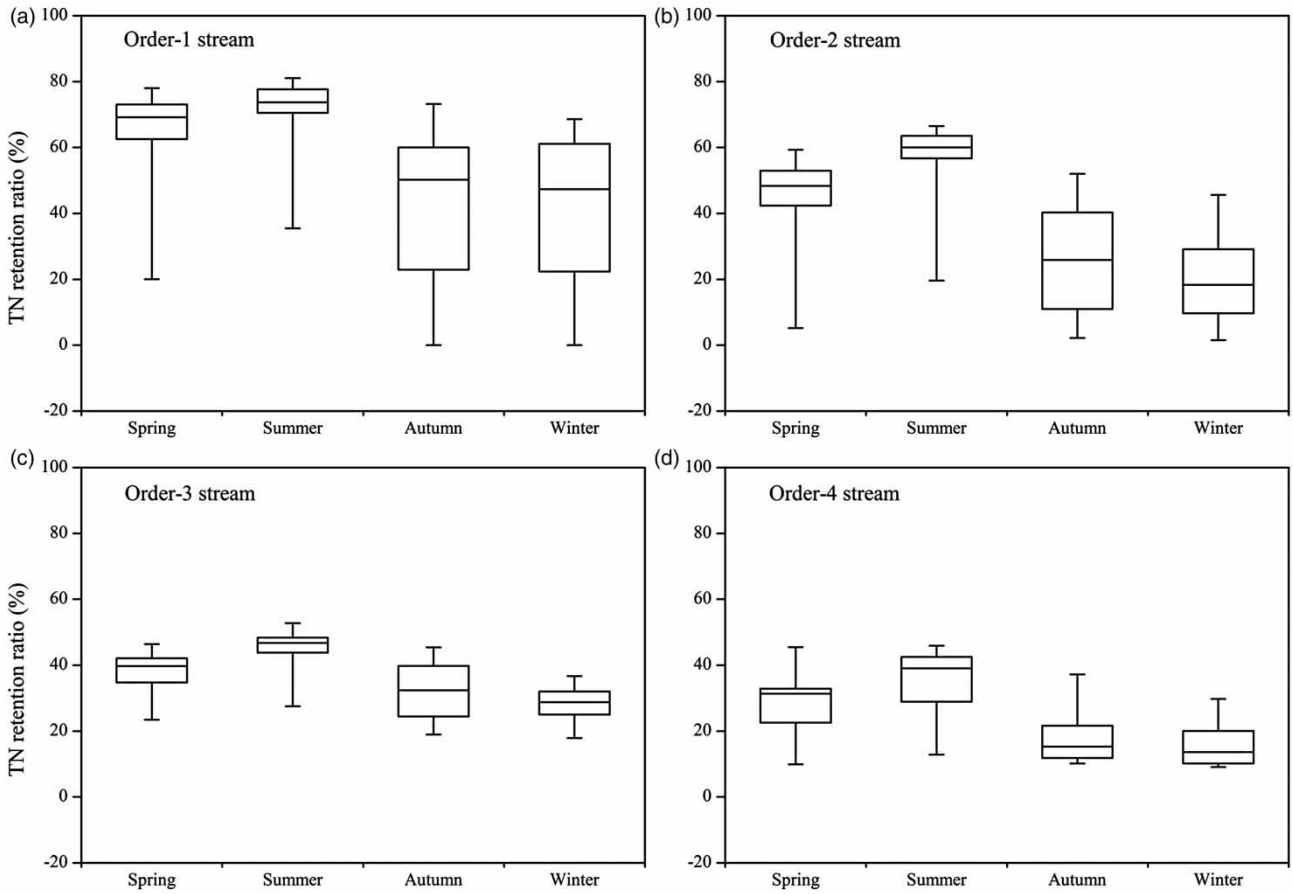

Figure 9 | Seasonal variations of the average TN retention ratios in streams of different orders (box plots display 2.5th, 25th, 50th, 75th, and 97.5th percentiles).

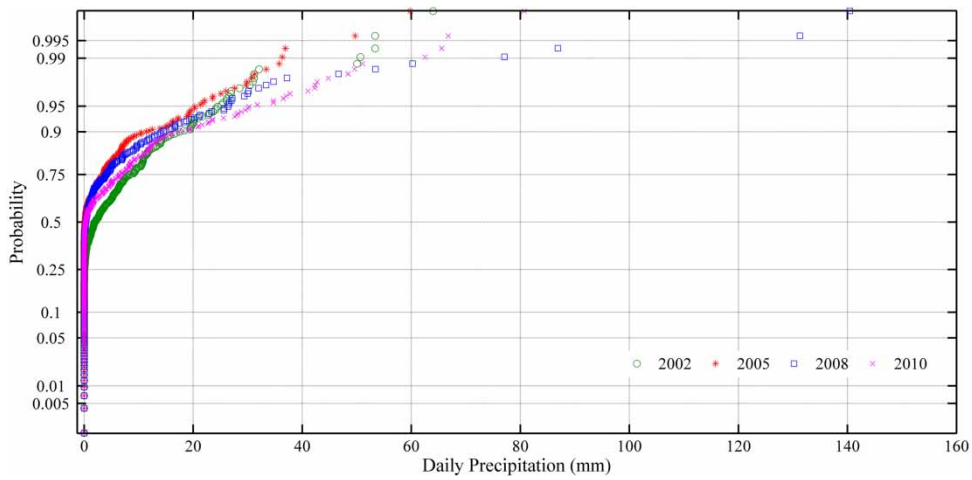

Figure 10 | Accumulative probability distribution of the daily precipitation in 2002, 2005, 2008, and 2010, respectively.

Downloaded from https://iwaponline.com/hr/article-pdf/47/4/869/368357/nh0470869.pdf
by guest
on 14 August 2018

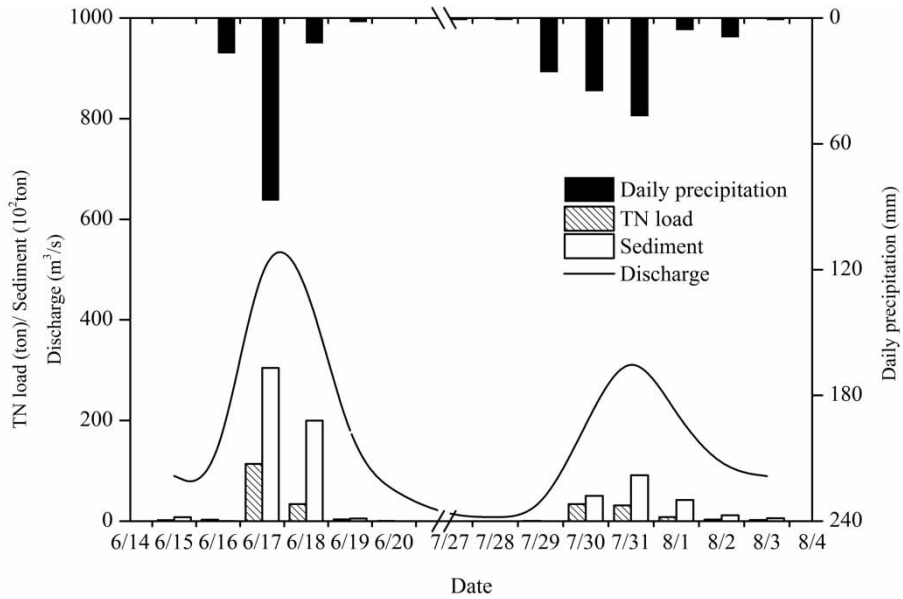

Figure 11 | Comparison of daily TN load, sediment, and discharge during two rainfall events in 2008 at Yuliang station.

Table 3 | Pearson correlation between the annual TN load and the area of each land use type

	Forest	Irrigated cropland	Upland	Grassland	Shrub	TN load
Forest	1	−0.768**	0.011	0.069	−0.333**	−0.427**
Irrigated cropland		1	−0.052	−0.339**	−0.126	0.688**
Upland			1	0.174	−0.038	0.109
Grassland				1	0.172	−0.246*
Shrub					1	−0.051
TN load						1

**Denotes significant relationship at a probability level of 0.01.
*Denotes significant relationship at a probability level of 0.05.

Control factor of TN retention in river network

No single factor is responsible for nutrient retention in lotic ecosystems; instead, this process is governed by complex interactions of abiotic and biotic processes (D'Angelo *et al.* 1991; Haggard *et al.* 2001). As mentioned before, TN retention is mainly caused by plant uptake and nitrate denitrification. Owing to the rapid growth of aquatic plants in summer, nitrate uptake increases in streams. At the same time, high air temperature leads to vigorous activities of microorganisms and reduces dissolved oxygen content in water, which may also accelerate the denitrification process. Although mineralization and nitrification can also be accelerated in summer, these processes can only change different N forms but the total amount of N will not be changed. Therefore, increased retention ratio in summer is mainly caused by the aquatic plant growth and microorganism action (D'Angelo & Webster 1991; Chen *et al.* 2010, 2013).

Table 4 lists the major hydro-morphological characteristics of streams in each order and their annual TN load from hillslopes and the TN retention ratios in streams. It can be used to analyze the major impact factors of retention ratios in addition to biological and chemical factors. The results show that the retention ratio has positive correlation with river length and negative correlation with discharge and velocity. It is also a fact that the increase of water

Downloaded from https://iwaponline.com/hr/article-pdf/47/4/869/368357/nh0470869.pdf
by guest
on 14 August 2018

Table 4 | Major hydro-morphological characteristics of streams in each order and the nitrogen retention ratios

		Average hydro-morphological characteristics						
Stream order	**Number of streams**	**Length (km)**	**Drainage area (km^2)**	**Longitudinal gradient (%)**	**Discharge (m^3/s)**	**Velocity (m/s)**	**Annual TN load (ton/km^2)**	**Retention ratio (%)**
1	39	17.80	94.48	20.75	2.67	0.12	0.86	37.53
2	17	13.22	67.94	9.81	10.25	0.15	1.12	21.36
3	16	8.84	44.94	6.37	43.64	0.24	1.20	19.26
4	5	7.35	68.00	21.40	153.10	0.59	1.16	4.31

residence time would enhance TN retention in the river network. Therefore, hydro-morphological characteristics, especially discharge and velocity, determine TN retention in streams of the study catchment. As mentioned above, the biological and chemical behavior in the streams also influences the TN retention, which should be analyzed carefully in future studies. For this purpose, other methods like ^{15}N-NO_3 tracer-addition approach (Mulholland *et al.* 2009) can be adopted.

Relationship between hillslope TN load and river retention

In addition to physical and biochemical properties of the streams, river TN retention is also closely related to TN load from the hillslopes. Therefore, it is important to know how the retention ratios change with the TN load from hillslopes. Owing to the limitation of observations, a scenario analysis is conducted to investigate the relationship between river TN retention and hillslope TN load in this catchment. For simplification in this study, it is assumed that the wetland is cultivated into irrigated cropland, other land use types are cultivated into upland and plantation except for the current urban area and water body, and that fertilizer is applied to all cropland and plantation areas homogeneously. Except for the original results, seven scenarios of fertilizer application were designed in this study: average value (200 kg/ha per year) of the present fertilizer application, and 1.5, 2, 4, 8, 16, and 32 times the present amount. Based on these designed fertilizer application scenarios, the GBNP model was run by using the same historic climate forcing data from 2001 to 2010 and the same model parameters calibrated in the above simulation of the actual case. Although this treatment would never happen in practice, it is a common method used in synthetic studies and is helpful to explore how the riverine TN retention would change with hillslope TN load.

Based on the simulated results, 10-year mean annual TN load and mean annual TN retention ratio for each stream of the different orders are calculated and plotted in Figure 12. It is shown that the retention ratio increases with the TN load but approaches a constant value when the TN load is large enough. The TN retention capacity decreases from the headstream (order 1 stream) to the stream of higher order. The maximum value of TN retention ratio is nearly 70% for streams of order 1, 60% for streams of order 2, 45% for order 3, and 50% for streams of order 4.

These maximum values of TN retention ratios should correspond to the self-purification capacity of the streams in this study catchment, which is potentially useful for making the nutrient mitigation measures. When the TN load is relatively lower, the retention ratios increase rapidly. It implies that the

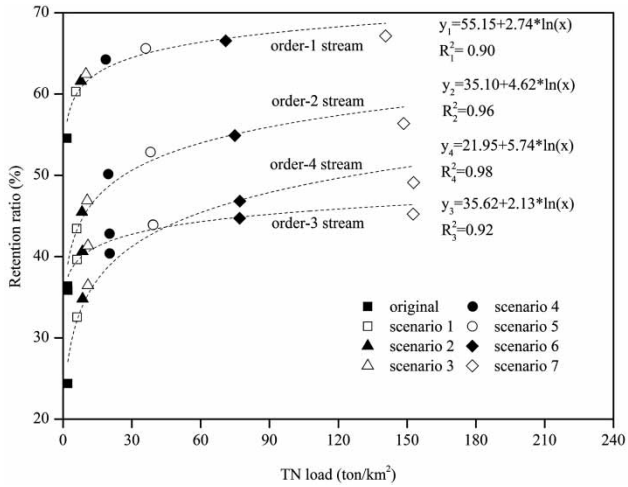

Figure 12 | Changes of retention ratios with TN load in streams of the different orders under different scenarios.

Downloaded from https://iwaponline.com/hr/article-pdf/47/4/869/368357/nh0470869.pdf
by guest
on 14 August 2018

rivers have active self-purification roles. However, when the TN load reaches a threshold, the self-purification may be decreased (Gasiūnas & Lysovienė 2014).

As shown in Figure 12, the TN retention ratio would sustain a stable value for a long time even when the TN load reached an extremely high value. However, in an actual case, there must be an upper limit of TN load into streams so that aquatic organisms can steady growth. When N is the limiting factor in this area at the beginning, with the increase of TN emissions, phytoplankton increases rapidly and takes up more nitrate. Meanwhile, the N/P ratios will increase. Once N/P ratio is greater than 20:1, the limiting factor will change into P (Schanz & Juon 1983). Then, the growth rate of phytoplankton will be reduced, and the uptake nitrate and the TN retention will be decreased consequently. The GBNP model could not simulate this process of the aquatic ecosystem, and this should be an important research topic in future study.

CONCLUSION

This paper uses the GBNP model to simulate rainfall–runoff, soil erosion, and TN load on hillslopes and river discharge, sediment, and TN transport in a river network in the upper XAJ catchment. The TN load from hillslope and TN retention in the river network were analyzed. The results lead to the following conclusions:

1. The GBNP model could simulate the monthly river discharge, sediment concentration, and TN concentration at an acceptable accuracy in the study catchment from 2001 to 2010. The R^2 values are greater than 0.9 for river discharge and sediment concentration, and are greater than 0.8 for TN concentration. The E_{ns} values for river discharge are greater than 0.8, except for the validation period in Linxi and Yuliang stations. The E_{ns} values for sediment and TN concentrations are smaller than those for river discharge (smallest value is 0.58).
2. Annual TN load from hillslopes varied from about 3,156 ton (0.54 ton/km^2) to 11,079 ton (1.88 ton/km^2) with a significant increasing trend during 2001–2010. Spring and summer are the major seasons for TN load and the highest TN load occurs in the central region of the study catchment. TN load has a significant positive correlation with both discharge and sediment. Precipitation may affect TN load, but the critical factor was proved to be rainfall intensity. The irrigated cropland is the major source of TN load in this catchment and the forest and grassland are demonstrated to be a sink.
3. The seasonal variations of TN retention ratio in the river network show that the retention ratio varied from 0% to 81% in the whole catchment. The highest retention ratio appeared in summer, due to the rapid growth of aquatic plants and vigorous activities of microorganisms, which accelerate plant uptake and denitrification process. In the river network, order 1 streams have the highest retention ratio followed by the orders 2, 3, and 4, which is mainly determined by the river hydraulic properties. In this research, retention ratio has a positive correlation with river length and negative correlation with discharge and velocity.
4. Nitrogen retention ratio increases logarithmically with the TN load for all streams of different orders based on scenario analysis. The maximum value of retention ratio is nearly 70% for order 1 streams, 60% for order 2 streams, 45% for order 3 streams, and 50% for order 4 streams. However, the TN retention ratio is also closely related to N/P ratios. When a change occurs in the limiting factor, the TN retention ratio will change consequently. Since these processes have not been described in the GBNP model, the maximum value of TN retention ratio might be overestimated in this study, and this needs further study in the future.

ACKNOWLEDGEMENTS

The research was supported by the National Natural Science Foundation of China (Project Nos 51025931 and 51139002).

REFERENCES

Alexander, R. B., Smith, R. A., Schwarz, G. E., Boyer, E. W., Nolan, J. V. & Brakebill, J. W. 2007 Differences in phosphorus and TN delivery to the Gulf of Mexico from the Mississippi River Basin. *Environ. Sci. Technol.* **42**, 822–830.

Downloaded from https://iwaponline.com/hr/article-pdf/47/4/869/368357/nh0470869.pdf
by guest
on 14 August 2018

Aravena, R., Auge, M. & Bucich, N. 1999 Evaluation of the origin of groundwater nitrate in the city La Plata–Argentina, using isotope techniques. *Hydrogeo. and Land Use Manag.* 323–327.

Behrendt, H. & Opitz, D. 2000 Retention of nutrients in river systems: dependence on specific runoff and hydraulic load. *Hydrobiologia* **400**, 111–222.

Bennett, J. P. 1974 Concepts of mathematical modeling of sediment yield. *Water. Resour. Res.* **10**, 485–492.

Bicknell, B. R., Imhoff, J. C., Kittle Jr, J. L., Donigian Jr, A. S. & Johanson, R. C. 1997 *Hydrological simulation program–Fortran: User's manual for version II*. US Environmental Protection Agency, National Exposure Research Laboratory, Athens, GA, USA.

Biggar, J. W. & Nielsen, D. R. 1962 Miscible displacement II behavior of tracers. *Soil Sci. Soc. Am. Proc.* **26**, 125–128.

Biggar, J. W. & Nielsen, D. R. 1963 Miscible displacement V: exchange processes. *Soil Sci. Soc. Am. Proc.* **27**, 623–627.

Borah, D. K. & Bera, M. 2004 Watershed-scale hydrologic and nonpoint-source pollution models: Review of applications. *T. ASABE* **47**, 789–803.

Brown, L. C. & Barnwell, T. O. 1987 *The enhanced stream water quality models QUAL2E and QUAL2E-UNCAS: documentation and user manual*. US Environmental Protection Agency. Office of Research and Development. Environmental Research Laboratory, Athens, GA, USA.

Cao, F., Li, X., Wang, D., Zhao, Y. & Wang, Y. 2013 Effects of land use structure on water quality in Xin'anjiang river. *Environ. Sci.* **34**, 2582–2587 (In Chinese).

Chen, D., Lu, J., Wang, H. & Shen, Y. N. 2010 Seasonal variations of TN and phosphorus retention in an agricultural drainage river in East China. *Environ. Sci. Pollut. R.* **17**, 312–320.

Chen, D., Dahlgren, R. A. & Lu, J. 2013 A modified load apportionment model for identifying point and diffuse source nutrient inputs to rivers from stream monitoring data. *J. Hydrol.* **501**, 25–34.

Chu, J. 1994 The impact way of scouring and sedimentation of river bottom sediment on water quality. *J. Hydraul. Eng.* **11**, 41–69 (In Chinese).

Collick, A. S., Fuka, D. R., Kleinman, P. J. A., Buda, A. R., Weld, J. L., White, M. J., Veith, T. L., Bryant, R. B., Bolster, C. H. & Easton, Z. M. 2015 Predicting phosphorus dynamics in complex terrains using a variable source area hydrology model. *Hydrol. Process.* **29** (4), 588–601.

Cong, Z., Yang, D., Gao, B., Yang, H. & Hu, H. 2009 Hydrological trend analysis in the Yellow River basin using a distributed hydrological model. *Water. Resour. Res.* **45**, W00A13, doi:10.1029/2008WR006852.

Covino, T., McGlynn, B. & Baker, M. 2010a Separating physical and biological nutrient retention and quantifying uptake kinetics from ambient to saturation in successive mountain stream reaches. *J. Geophys. Res.* **115**, G04010, doi:10.1029/2009JG001263.

Covino, T., McGlynn, B. & McNamara, R. 2010b Tracer Additions for Spiraling Curve Characterization (TASCC): Quantifying stream nutrient uptake kinetics from ambient to saturation. *Limnol. Oceanogr-Meth.* **8**, 484–498.

Dai, Y., Shangguan, W., Duan, Q., Liu, B., Fu, S. & Niu, G. 2013 Development of a China dataset of soil hydraulic parameters using pedotransfer functions for land surface modeling. *J. Hydrometeorol.* **14**, 869–887.

D'Angelo, D. J. & Webster, J. R. 1991 Phosphorus retention in streams draining pine and hardwood catchments in the Southern Appalachian Mountains. *Freshwater Bio.* **26**, 35–45.

D'Angelo, D. J., Webster, J. R. & Benfield, E. F. 1991 Mechanisms of stream phosphorus retention: an experimental study. *J. N. Am. Benthol. Soc.* **10**, 225–237.

Environmental Monitor Station of Huangshan 2011 *Environmental quality report of Huangshan from 2006 to 2010*. Environmental Protection Agency of Huangshan, China (In Chinese).

Esen, E. & Uslu, O. 2008 Assessment of the effects of agricultural practices on non-point source pollution for a coastal watershed: a case study Nif Watershed, Turkey. *Ocean. Coastal. Manage.* **51**, 601–611.

Gao, B., Todd Walter, M., Steenhuis, T. S., Hogarth, W. L. & Parlange, J. 2004 Rainfall induced chemical transport from soil to runoff: theory and experiments. *J. Hydrol.* **295**, 291–304.

Gasiūnas, V. & Lysovienė, J. 2014 Nutrient retention efficiency of small regulated streams during the season of low-flow regime in Central Lithuanian lowland. *Hydrol. Res.* **45** (3), 357–367.

Grizzetti, B., Bouraoui, F., Granlund, K., Rekolainen, S. & Bidoglio, G. 2003 Modelling diffuse emission and retention of nutrients in the Vantaanjoki watershed (Finland) using the SWAT model. *Ecol. Model.* **169**, 25–38.

Haggard, B. E., Storm, D. E. & Stanley, E. H. 2001 Effect of a point source input on stream nutrient retention. *J. Am. Water Resour. Ass.* **37** (5), 1291–1299.

Kronvang, B., Hoffmann, C. C., Svendsen, L. M., Windolf, J., Jensen, J. P. & Dørge, J. 1999 Retention of nutrients in river basins. *Aquat. Ecol.* **33**, 29–40.

Li, Z. L., Lv, Z. F., Zhao, Y., Wang, Y. Q. & Zhang, Z. 2015 Construction of SWAT model and its applicability in upper basin of Xin'an River. *J. Water. Resour. Water. Eng.* **26** (1), 25–30 (In Chinese).

Libra, R. D. & Hallberg, G. R. 1998 Impacts of agriculture on water quality in the Big Spring Basin, NE Iowa, U.S.A. *Karst Hydrogeology and Human Activities. Australia* **1**, 57–58.

Liu, Y. 2009 Investigation and evaluation of groundwater pollution and its control research for Anhui province. Master dissertation, Hefei University of Technology, China (In Chinese).

Ma, H., Yang, D., Tan, S., Gao, B. & Hu, Q. 2010 Impact of climate variability and human activity on streamflow decrease in the Miyun Reservoir catchment. *J. Hydrol.* **389**, 317–324.

Mao, Z., Shan, B., Peng, W. & Wang, H. 2006 Advances in research on nitrogen retention in river ecosystems. *Resour. Environ. Yangtze Basin* **15** (4), 480–484 (In Chinese).

Downloaded from https://iwaponline.com/hr/article-pdf/47/4/869/368357/nh0470869.pdf
by guest
on 14 August 2018

McBroom, M. W., Beasley, R. S., Chang, M. & Ice, G. G. 2008 Storm runoff and sediment losses from forest clearcutting and stand re-establishment with best management practices in East Texas, USA. *Hydrol. Process.* **22**, 1509–1522.

McNamara, R. A. 2010 *Stream TN uptake dynamics from ambient to saturation across development gradients, stream network position, and seasons*. College of Agriculture, Montana State University, Bozeman, MT, USA.

Mulholland, P. J., Helton, A. M., Poole, G. C., Hall, R. O., Hamilton, S. K., Peterson, B. J., Tank, J. L., Ashkenas, L. R., Cooper, L. W., Dahm, C. N., Dodds, W. K., Findlay, S. E., Gregory, S. V., Grimm, N. B., Johnson, S. L., McDowell, W. H., Meyer, J. L., Valett, H. M., Webster, J. R., Arango, C. P., Beaulieu, J. J., Bernot, M. J., Burgin, A. J., Crenshaw, C. L., Johnson, L. T., Niederlehner, B. R., O'Brien, J. M., Potter, J. D., Sheibley, R. W., Sobota, D. J. & Thomas, S. M. 2008 Stream denitrification across biomes and its response to anthropogenic nitrate loading. *Nature* **452**, 202–205.

Mulholland, P. J., Hall, R. O., Sobota, D. J., Dodds, W. K., Findlay, S. E. G., Grimm, N. B., Hamilton, S. K., McDowell, W. H., O'Brien, J. M., Tank, J. L., Ashkenas, L. R., Cooper, L. W., Dahm, C. N., Gregory, S. V., Johnson, S. L., Meyer, J. L., Peterson, B. J., Poole, G. C., Valett, H. M., Webster, J. R., Arango, C. P., Beaulieu, J. J., Bernot, M. J., Burgin, A. J., Crenshaw, C. L., Helton, A. M., Johnson, L. T., Niederlehner, B. R., Potter, J. D., Sheibley, R. W. & Thomas, S. A. 2009 Nitrate removal in stream ecosystems measured by 15N addition experiments: denitrification. *Limnol. Oceanogr.* **54** (3), 666–680.

Neilsen, D. R. & Biggar, J. W. 1961 Miscible displacement in soils: Experimental information. *Soil Sci. Soc. Am. Proc.* **25**, 1–5.

Neilsen, D. R. & Biggar, J. W. 1962 Miscible displacement in soil: III Theoretical consideration. *Soil Sci. Soc. Am. Proc.* **26**, 216–221.

Ongley, E. D., Zhang, X. L. & Yu, T. 2010 Current status of agricultural and rural non-point source pollution assessment in China. *Environ. Pollut.* **158**, 1159–1168.

Ouyang, W., Wang, X., Hao, F. & Srinivasan, R. 2009 Temporal-spatial dynamics of vegetation variation on non-point source nutrient pollution. *Ecol. Model.* **220**, 2702–2713.

Peterson, B. J., Wollheim, W. M., Mulholland, P. J., Webster, J. R., Meyer, J. L., Tank, J. L., Marti, E., Bowden, W. B., Vallett, H. M., Hershey, A. E., McDowell, W. H., Dodds, W. K., Hamilton, S. K., Gregory, S. & Morall, D. D. 2001 Control of TN export from watersheds by headwater streams. *Science* **292**, 86–90.

Pimentel, D. 1993 *World Soil Erosion and Conservation*. No. GTZ-PR 544. Cambridge University Press, Cambridge.

Rankinen, K., Granlund, K., Etheridge, R. & Seuri, P. 2014 Valuation of nitrogen retention as an ecosystem service on a catchment. *Hydrol. Res.* **45** (3), 411–424.

Saunders, D. L. & Kalff, J. 2001 TN Retention in wetlands, lakes and rivers. *Hydrobiologia* **443**, 205–212.

Schanz, F. & Juon, H. 1983 Two different methods of evaluating nutrient limitation of periphyton bioassays using water from the River Rhine and eight of its tributaries. *Hydrobiologia* **102**, 187–195.

Seitzinger, S. P., Styles, R. V., Boyer, E. W., Alexander, R. B., Billen, G., Howarth, R. W., Mayer, B. & Van Breemen, N. 2002 Nitrogen retention in rivers: model development and application to watershed in the northeastern U.S.A. *Biogeochem.* **57/58**, 199–237.

Shen, Z., Chen, L., Liao, Q., Liu, R. & Hong, Q. 2012 Impact of spatial rainfall variability on hydrology and nonpoint source pollution modeling. *J. Hydrol.* **472**, 205–215.

Shen, Z., Chen, L., Hong, Q., Qiu, J., Xie, H. & Liu, R. 2013 Assessment of TN and phosphorus loads and causal factors from different land use and soil types in the Three Gorges Reservoir Area. *Sci. Total. Environ.* **454**, 383–392.

Shen, Z., Qiu, J., Hong, Q. & Chen, L. 2014 Simulation of spatial and temporal distributions of non-point source pollution load in the Three Gorges Reservoir Region. *Sci. Total. Environ.* **493**, 138–146.

Somura, H., Takeda, I., Arnold, J. G., Mori, Y., Jeong, J., Kannan, N. & Hoffman, D. 2012 Impact of suspended sediment and nutrient loading from land uses against water quality in the Hii River basin, Japan. *J. Hydrol.* **450**, 25–35.

Spieles, D. J. & Mitsch, W. J. 1999 The effects of season and hydrologic and chemical loading on nitrate retention in constructed wetlands: a comparison of low- and high-nutrient riverine systems. *Ecol. Eng.* **14**, 77–91.

Statistics Office of Huangshan 2011 *The Statistics Yearbook of Huangshan*. Huangshan Publishing House, China (In Chinese).

Svendsen, L. M. & Kronvang, B. 1993 Retention of TN and phosphorus in a Danish lowland river system: implications for the export from the watershed. *Hydrobiology* **82**, 123–135.

Tang, L., Yang, D., Hu, H. & Gao, B. 2011 Detecting the effect of land-use change on streamflow, sediment and nutrient losses by distributed hydrological simulation. *J. Hydrol.* **409**, 172–182.

Wang, G. Q. & Hu, C. H. 2006 *Advance in Sediment Research*. China Water Power Press, Beijing, China (In Chinese).

Wang, X. L., Wang, Q., Wu, C. Q., Liang, T., Zheng, D. H. & Wei, X. F. 2012 A method coupled with remote sensing data to evaluate non-point source pollution in the Xin'anjiang catchment of China. *Sci. Total. Environ.* **430**, 132–143.

Wang, A., Tang, L. H., Wang, T. T. & Yang, D. W. 2014 Simulation of non-point source pollution in the upper basin of Xin'anjiang catchment using GBNP model. *J. Hydraul. Eng.* **45** (11), 1–15 (In Chinese).

Watts, D. G. & Hanks, R. J. 1978 A soil-water-nitrogen model for irrigated corn on sandy soils. *Soil Sci. Soc. Am. J.* **42**, 492–499.

Wu, L., Long, T., Liu, X. & Guo, J. S. 2012 Impacts of climate and land-use changes on the migration of non-point source TN and phosphorus during rainfall-runoff in the Jialing River Watershed, China. *J. Hydrol.* **475**, 26–41.

Xu, J., Yang, D., Yi, Y., Lei, Z., Chen, J. & Yang, W. 2008 Spatial and temporal variation of runoff in the Yangtze River basin during the past 40 years. *Quatern. Int.* **186**, 32–42.

Yang, D., Herath, S. & Musiake, K. 1998 Development of a geomorphology-based hydrological model for large catchments. *Annu. J. Hydraul. Eng. JSCE* **42**, 169–174.

Downloaded from https://iwaponline.com/hr/article-pdf/47/4/869/368357/nh0470869.pdf
by guest
on 14 August 2018

Yang, D., Herath, S. & Musiake, K. 2002 A hillslope-based hydrological model using catchment area and width functions. *Hydrol. Sci. J.* **47**, 49–65.

Yang, D., Gao, B., Jiao, Y., Lei, H., Zhang, Y., Yang, H. & Cong, Z. 2015 A distributed scheme developed for eco-hydrological modeling in the upper Hei River. *Sci. China* **58**, 36–45.

Ye, C. & Wu, X. 2005 Effect of agricultural of non-point source pollution on water quality of Xin'an Jiang basin. *Anhui Agri. Sci. Bull.* **11**, 158 (In Chinese).

Ye, S., Covino, T. P., Sivapalan, M., Basu, N. B., Li, H. & Wang, S. 2012 Dissolved nutrient retention dynamics in river networks: A modeling investigation of transient flows and scale effects. *Water. Resour. Res.* **48**, W00J17, doi: 10.1029/2011wr010508.

Young, R. A., Onstad, C. A., Bosch, D. D. & Anderson, W. P. 1989 AGNPS: A nonpoint-source pollution model for evaluating agricultural watersheds. *J. Soil. Water. Conserv.* **44**, 168–173.

Yu, X., Yang, Z., Zhong, D. & Peng, Q. 2006 Numerical model for interaction between sediment and pollutant in river. *J. Hydraul. Eng.* **37**, 10–15 (In Chinese).

Zhai, X., Zhang, Y., Wang, X., Xia, J. & Liang, T. 2014 Non-point source pollution modelling using Soil and Water Assessment Tool and its parameter sensitivity analysis in Xin'anjiang catchment, China. *Hydrol. Process.* **28**, 1627–1640.

Zhang, G., Chen, H., Zhang, J. & Liu, S. 2003 Nutrient element in the atmospheric wet deposition in Changjiang River estuary. *Chinese J. Appl. Ecol.* **14** (7), 1107–1111 (In Chinese).

First received 23 March 2015; accepted in revised form 23 June 2015. Available online 31 July 2015

Downloaded from https://iwaponline.com/hr/article-pdf/47/4/869/368357/nh0470869.pdf
by guest
on 14 August 2018